Droplet evaporation: A molecular dynamics investigation

E. S. Landry, S. Mikkilineni, M. Paharia, and A. J. H. McGaughey[a)]
Department of Mechanical Engineering, Carnegie Mellon University, Pittsburgh, Pennsylvania 15213, USA

(Received 29 August 2007; accepted 15 October 2007; published online 17 December 2007)

Molecular dynamics simulations are used to model the evaporation of a Lennard–Jones argon nanodroplet into its own vapor for a wide range of ambient temperatures and ambient pressures. The transitions from (i) high to low Knudsen number evaporation and (ii) subcritical to supercritical evaporation are observed. At a low ambient pressure of 0.4 MPa, the initial droplet Knudsen number is 1 and the droplet diameter decreases linearly with time, consistent with kinetic theory predictions. For a moderate ambient pressure of 3.0 MPa, the initial droplet Knudsen number is 0.1 and the square of the droplet diameter decreases linearly with time. For a high ambient pressure of 6.1 MPa, the evaporation is supercritical and the number of atoms in the droplet decreases linearly for the majority of the droplet lifetime. A technique is introduced to maintain a constant ambient pressure over the droplet lifetime, allowing for the observation of the influence of the ambient conditions on the droplet surface temperature. When the ambient pressure is greater than or equal to 1.4 times the critical pressure, the droplet surface temperature reaches the critical temperature and the evaporation is supercritical. Below this ambient pressure, the droplet surface temperature reaches a pseudowet-bulb condition. © *2007 American Institute of Physics*. [DOI: 10.1063/1.2821753]

I. INTRODUCTION

The ability to predict droplet evaporation rates is important in diverse applications such as spray combustion, spray cooling, and the delivery of medical aerosols to the lungs.[1] The droplet evaporation rate is influenced by the droplet Knudsen number (Kn) defined as[1,2]

$$\mathrm{Kn} = \frac{\lambda}{D}, \tag{1}$$

where λ is the atomic mean free path near the droplet surface and D is the droplet diameter. In the continuum regime (i.e., $\mathrm{Kn} \ll 0.1$), by assuming that (i) the droplet surface temperature is below the critical temperature (i.e., subcritical evaporation), (ii) the liquid and vapor phases are quasisteady, (iii) the droplet remains spherical throughout its lifetime, and (iv) the evaporation occurs in an environment with negligible forced or natural convection, hydrodynamic theory can be used to develop the D^2 law.[2,3] This model predicts the time rate of change of the square of the droplet diameter to be constant, i.e.,

$$\frac{dD^2}{dt} = -K, \tag{2}$$

where t is time and K is the evaporation constant. The evaporation behavior is significantly different, however, in the free molecular regime (i.e., $\mathrm{Kn} \gg 1$). In this regime, kinetic theory-based models (e.g., the Hertz–Knudsen–Langmuir equation) predict the droplet diameter to decrease linearly with time, assuming that the liquid and vapor phases are quasisteady and that the incoming and outgoing velocity distributions in the vapor are Maxwellian.[1,4] For intermediate values of the Knudsen number (i.e., the transitional regime), theoretical prediction of the evaporation requires solutions to the Boltzmann equation.[5]

The models for droplet evaporation developed for the transitional and free molecular regimes often require knowledge of phenomenological parameters (e.g., evaporation and condensation coefficients in the Hertz–Knudsen–Langmuir equation) or assumptions about the intensity of the evaporation (e.g., a low Mach number in the vapor is required to assume a Maxwellian velocity distribution). These parameters and assumptions limit the usefulness of such models for practical applications. Similar challenges exist for models developed for the continuum regime. For example, D^2 law-type models are invalid for supercritical evaporation (i.e., droplet surface temperatures approaching the critical temperature) because the vapor and liquid phases become unsteady, and the surface tension goes to zero, reducing the validity of the spherical droplet assumption. Because many combustion systems operate at temperatures and pressures a factor of 2 or more times the critical properties of the fuel, supercritical evaporation is a possibility and accurate models for droplet evaporation are needed.[6]

Molecular dynamics (MD) simulations are a promising tool for modeling droplet evaporation because no *a priori* assumptions need to be made about the thermodynamic properties or behavior of the system once an appropriate interatomic potential is specified. Previous investigations have used MD to predict the evaporation of Lennard–Jones (LJ) nanodroplets (i.e., droplets with initial diameters of a few nanometers) into a surrounding vapor of the same species,[7–11] a vapor of a different species,[12,13] or a vacuum.[14] Long *et al.*[8] examined subcritical evaporation with an initial Knudsen number of 2 (details related to the estimation of the initial Knudsen numbers are provided in Sec. III B 1) and predicted the droplet diameter to decrease linearly with time, consistent with kinetic theory-based predictions. Little[9] ex-

[a)]Electronic mail: mcgaughey@cmu.edu.

amined subcritical evaporation with an initial Knudsen number of 0.07 and found the MD and D^2 law predictions of the evaporation rate to agree to within 20%. Walther and Koumoutsakos[7] considered subcritical evaporation with initial Knudsen numbers between 0.04 and 0.09 at the same ambient conditions examined by Little. These authors found that the MD prediction of the evaporation rate approaches the D^2 law prediction as the droplet size increased. We will show in Sec. III B, however, that Little[9] and Walther and Koumoutsakos[7] calculated the evaporation coefficient using an inappropriate reference temperature. Using the correct reference temperature leads to a greater difference between the MD and D^2 law predictions. Little[9] also examined supercritical nanodroplet evaporation and found that the droplet lost its sphericity due to the diminishing surface tension. Sumardiono and Fischer[10] predicted the subcritical evaporation of a nanodroplet with an initial Knudsen number of 0.5 and found that D^γ decreased linearly with time where γ was between 3.0 and 4.5. A possible explanation for this unexpected result is provided in Sec. III B 3. In a separate investigation, Sumardiono and Fischer[14] examined the evaporation of a nanodroplet initially exposed to a vacuum (the pressure far from the droplet increased from zero as the droplet evaporated). They found that the system eventually achieved an equilibrium state that can be predicted from the first law of thermodynamics. Consolini *et al.*[13] studied the subcritical and supercritical evaporation of cold xenon nanodroplets into initially hot nitrogen environments. For the subcritical case, it was found that an initially nonspherical droplet quickly became spherical, while for the supercritical case, the droplet never regained its sphericity due to the lack of surface tension. Kaltz *et al.*[12] studied the subcritical and supercritical evaporation of liquid oxygen nanodroplets into helium and hydrogen environments. These authors found that the droplet surface tension decreases as the ambient pressure increases and that pressures much higher than the critical pressure of oxygen were required for supercritical evaporation to occur.

Here, we will study the evaporation of LJ argon nanodroplets into their own vapor for a larger range of ambient temperatures and pressures than what has been considered by other authors. This range will allow the observation of the transitions from (i) high to low Knudsen number evaporation and (ii) subcritical to supercritical evaporation. The influence of the ambient temperature and pressure on the droplet surface temperature is also examined. A technique for maintaining a constant ambient pressure over the course of the simulation is introduced.

II. MOLECULAR DYNAMICS SIMULATIONS

A. Interatomic potential and simulation details

In a MD simulation, the time history of the positions and velocities of a set of atoms are predicted using the Newtonian equations of motion. In this investigation, the atomic interactions are modeled using the LJ 12–6 pair potential, where the potential energy, $\phi_{ij}(r_{ij})$, between two atoms, i and j, separated by a distance r_{ij} is given by

$$\phi_{ij}(r_{ij}) = 4\epsilon_{\mathrm{LJ}}\left[\left(\frac{\sigma_{\mathrm{LJ}}}{r_{ij}}\right)^{12} - \left(\frac{\sigma_{\mathrm{LJ}}}{r_{ij}}\right)^{6}\right], \tag{3}$$

where σ_{LJ} and ϵ_{LJ} are the zero-energy pair separation distance and potential well depth ($\epsilon_{\mathrm{LJ}}=1.67\times10^{-21}$ J, and $\sigma_{\mathrm{LJ}}=3.40\times10^{-10}$ m).[15] The mass scale, m_{LJ}, is 6.63×10^{-26} kg, the mass of one argon atom. The LJ potential has been used extensively in previous investigations of nanoscale thermal transport in solid and fluid phases.[7–10,12–14,16–23] Its simple form allows for fast simulations and for the elucidation of phenomena and development of analysis techniques that would not be possible in more complicated systems. A truncated and shifted cutoff scheme is used with a cutoff radius of $2.5\sigma_{\mathrm{LJ}}$ and a time step of $0.005\sqrt{\sigma_{\mathrm{LJ}}^2 m_{\mathrm{LJ}}/\epsilon_{\mathrm{LJ}}}$ (10.7 fs). Periodic boundary conditions are imposed in all directions, and the equations of motion are integrated using the velocity Verlet algorithm.

The initial system configuration for all simulations is a spherical droplet at equilibrium with its vapor. This configuration was created from the output of separate liquid-only and vapor-only simulations. Both of these simulations contained 1372 atoms in a cubic simulation cell with a cell length chosen in order to achieve densities of 1230 $\mathrm{kg/m^3}$ for the liquid and 33.4 $\mathrm{kg/m^3}$ for the vapor. These densities correspond to the saturated vapor and liquid densities at a temperature of 97 K. The saturation properties referred to throughout this work correspond to the data obtained from single phase simulations of the LJ fluid by Vrabec *et al.*[24] using the same cutoff scheme that we implemented. Our single phase simulations were run in the constant mass, volume, and energy ensemble at the saturation temperature for 100 000 time steps. This equilibration period was found to be sufficient to obtain Maxwellian statistics. The droplet was created by cutting the largest possible sphere from the liquid simulation output and the vapor was created by cutting a spherical hole of the same size from the vapor simulation output. The droplet was then combined with the vapor. At this point, the distance between all droplet and vapor atom pairs was calculated. If any distance was less than $0.9\sigma_{\mathrm{LJ}}$ (the start of the first peak in the radial distribution function) either the droplet or vapor atom was randomly deleted so as to prevent the system from starting with any large forces. The resulting configuration was then run for an additional 250 000 time steps with the positions and momenta of each atom printed to separate files every 10 000 time steps after the 200 000 time step mark. During the period where the atomic positions and momenta were being outputted, there was no significant change in the droplet mass, indicating that the droplet was in equilibrium with the vapor. Using this procedure, we created five separate input files for use as the initial conditions for the evaporation simulations. All data presented in this work are the average results obtained by running identical simulations with each of these five input files. The average initial droplet diameter is 4.6 nm (673 atoms), and the droplet is in equilibrium with its vapor containing 1418 atoms at a temperature of 93 K. A snapshot of one of the input files is shown in Fig. 1. Note that the droplet

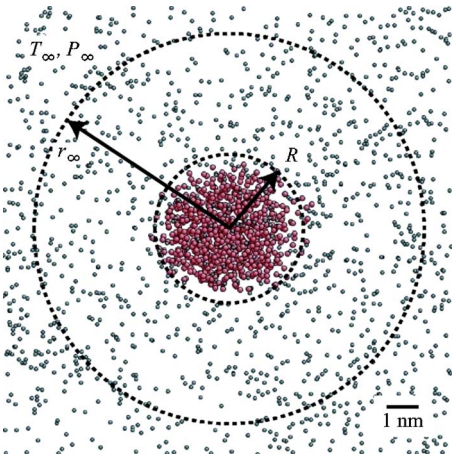

FIG. 1. (Color online) One of the five initial droplet configurations. All of the initial configurations are a droplet in equilibrium with its vapor at a temperature of 93 K. The droplet and vapor atoms are treated identically in the simulations and are shown with different colors for illustration purposes only.

and vapor atoms are shown with different colors for illustration purposes only. The atoms are treated identically in the simulations.

B. Ambient temperature and pressure control

The ambient pressure, P_∞, and temperature, T_∞, are controlled beyond a radius r_∞ from the center of the droplet (see Fig. 1). An r_∞ value of $18\sigma_{LJ}$ was found to be sufficient to eliminate any effects on the evaporation of the droplet and to have enough atoms in the ambient region so that the control schemes do not significantly affect the system dynamics.

The ambient temperature is kept constant over the course of the simulation through velocity rescaling. The ambient pressure is controlled by randomly deleting an atom in the ambient region when the ambient density, ρ_∞, becomes too high or by adding an atom when the ambient density becomes too low. When adding an atom, the randomly chosen location is first checked to see if there are any atoms within $1.12\sigma_{LJ}$ [the location of the minimum in Eq. (3)] of the location. This step is done to avoid sudden changes in the forces on the atoms. If the location fails this criterion, then a new location is chosen. The ambient density is allowed to fluctuate between $0.99\rho_\infty$ and $1.01\rho_\infty$ to minimize the effect of the pressure control on the natural system dynamics. We note that other authors[7,8,10,12–14] have allowed the ambient pressure to increase over the course of the simulation as atoms leave the droplet and enter the vapor. The droplet surface temperature and evaporation behavior, however, depend strongly on the ambient pressure (see Sec. III), especially when the droplet Knudsen numbers are large. Therefore, for our work, it is crucial to be able to accurately set the ambient pressure.

The addition and deletion of atoms over the course of the simulation causes the system momentum to not be conserved, leading to a required correction to the atomic velocities during the temperature calculation (discussed in Sec. II C). The ambient control scheme also leads to some unrealistic behavior at the start of the simulation due to an initially high pressure gradient that exists at the boundary to the ambient region. This pressure gradient drives a flow of atoms from the ambient region toward the droplet. A similar flux of mass from the far-field region toward the droplet was also observed by Sumardiono and Fischer.[10] This behavior is most extreme for high ambient pressure simulations where it can take 30% of the droplet lifetime (defined as the amount of time for the droplet to fully evaporate) for this flow to diminish. Because this is an artificial flow generated by the ambient control scheme, we disregard this portion of the droplet lifetime for all analyses.

C. Property measurement

The droplet size is determined at every time step using the Amsterdam method described by Sumardiono and Fischer[10,14] which is a slight modification to a method introduced by Rein ten Wolde and Frenkel.[25] This method is based on counting the number of atoms in the droplet, N_d. An atom is considered to be in the droplet if there are at least four other atoms within a distance of $1.5\sigma_{LJ}$. We then determine the droplet radius, R, by finding the minimum distance from the droplet center of mass that contains N_d atoms.

The droplet surface, droplet core, and ambient temperatures are also calculated at every time step. The atoms located within $R/2$ of the center of the droplet are considered to be in the core region and the rest of the droplet atoms are in the surface region. Two corrections must be made to the atomic velocities before calculating the temperature. First, the velocity associated with the drift of the system's center of mass (a consequence of the ambient control scheme discussed in Sec. II B) must be subtracted from the velocity of each atom. The second correction is made to account for the radial drift velocity of evaporated atoms as they move away from the droplet, which should not be included in the temperature calculation. We use the procedure outlined by Sumardiono and Fischer[14] for this correction.

III. RESULTS AND DISCUSSION

A. Influence of ambient temperature and pressure on droplet surface temperature

The critical temperature and density of LJ argon are 130 K and 538 kg/m^3.[24] We find that these conditions correspond to a critical pressure of 4.1 MPa. We consider reduced ambient temperatures (T_∞/T_{cr}) between 2.3 and 6.1, spanning a range relevant to the evaporation of hydrocarbon droplets in a combustor. The reduced ambient pressure (P_∞/P_{cr}) ranges from 0.1 to 1.5, allowing for the examination of evaporation behavior with droplet surface temperatures both above and below the critical temperature.

The time history of the droplet surface temperature is shown in Fig. 2 for ambient pressures of 0.4, 1.1, 3.0, and 6.1 MPa, and an ambient temperature of 500 K. This ambient temperature is moderate for the range we examined and provides a good representation of the types of behavior observed in this study. The plotted time has been normalized by the droplet lifetime, τ_d, so that all three cases can be compared on the same plot. For the low ambient pressure case of 0.4 MPa, the droplet surface temperature initially decreases be-

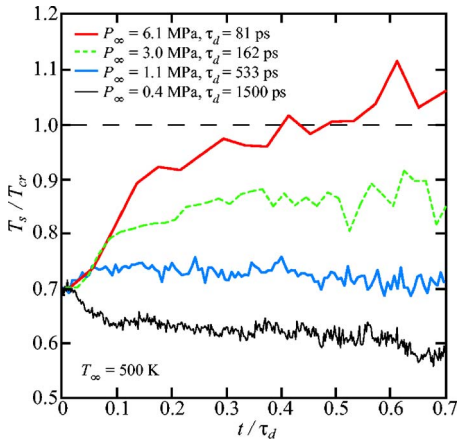

FIG. 2. (Color online) Time histories of the droplet surface temperature for an ambient temperature of 500 K and ambient pressures of 0.4, 1.1, 3.0, and 6.1 MPa. The plotted time has been normalized by the droplet lifetime, τ_d, and each data point is an average over 3.21 ps (300 time steps).

cause the ambient pressure is lower than the initial pressure. After $t/\tau_d \simeq 0.1$, the surface temperature reaches a pseudowet-bulb temperature. The wet-bulb temperature describes the state where the droplet heating is zero and all heat conducted from the vapor to the droplet is used for the phase change. As suggested by Givler and Abraham,[6] the term pseudowet-bulb temperature is used because the droplet temperature is never exactly uniform and therefore, will always be in a transient state. For ambient pressures of 1.1 and 3.0 MPa, the surface temperature initially increases and then reaches a pseudowet-bulb temperature that is below the critical temperature after $t/\tau_d \simeq 0.1$ and $t/\tau_d \simeq 0.3$. For the high ambient pressure case of 6.1 MPa, the surface temperature increases to a value greater than the critical temperature and is transient over the entire droplet lifetime. The observation that the droplet spends a greater fraction of its lifetime in a transient heating period as the ambient pressure increases is in qualitative agreement with experimental studies of evaporating hydrocarbon droplets.[6]

The predicted reduced droplet surface temperature (T_s/T_{cr}) is shown as function of reduced ambient pressure in Fig. 3 for the full range of ambient temperatures. The plotted surface temperature is the temporal average between the time that the droplet reaches a pseudowet-bulb temperature and when there are 100 atoms left in the droplet. In all of these cases, this time period is at least 36 ps (3400 time steps), a duration that we believe to be sufficient to specify the surface temperature to within 2 K. The droplet surface temperature is dependent only on the ambient pressure. In all cases, the droplet surface temperature is below the saturation temperature at the ambient pressure and the difference between these temperatures increases with increasing ambient pressure. The droplet surface temperature data for reduced ambient pressures above 0.7 has been fit to a line using a least-squares analysis. Extrapolating this linear function to the point where the droplet surface temperature is equal to the critical temperature gives an ambient pressure equal to 1.4 times the critical pressure. For ambient pressures above this value, supercritical evaporation is expected.

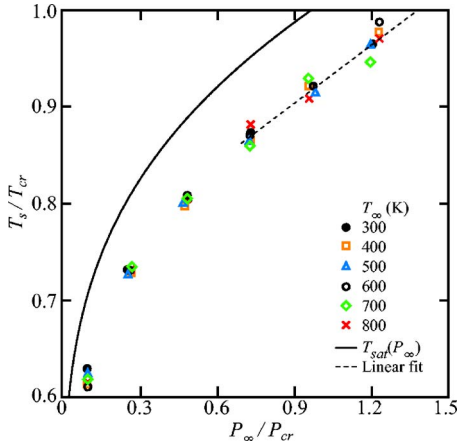

FIG. 3. (Color online) Reduced droplet surface temperature plotted against the reduced ambient pressure.

B. Predicted evaporation behavior and comparison with theory

1. Estimation of the droplet Knudsen number and D^2 law calculation of the evaporation rate

In the next four sections, we describe the predicted evaporation behavior at the low, moderate, and high ambient pressures of 0.4, 3.0, and 6.1 MPa. We observed significantly different behavior between these ambient pressures, which we attribute to the differences in initial Knudsen numbers and the droplet surface temperature. The Knudsen numbers provided throughout this paper are calculated using Eq. (1), the initial droplet diameter, and by estimating the atomic mean free path to be[26]

$$\lambda = \frac{1}{\sqrt{2}\pi d^2 n_v}, \tag{4}$$

where d is the effective atomic diameter and n_v is the atomic number density of the vapor near the droplet surface. The atomic diameter is taken as σ_{LJ} and the number density near the droplet surface is estimated as the saturated vapor density at the ambient pressure.

For the low and moderate pressure cases, we compare the MD predictions to the evaporation rates calculated from the D^2 law. The D^2 law evaporation constant, K, can be predicted from the conservation equations to be[3,27]

$$K = \frac{8k^V}{\rho^L c_p^V} \ln\left[1 + \frac{c_p^V (T_\infty - T_s)}{h_{LV} + \dot{Q}_L/\dot{m}}\right], \tag{5}$$

where the superscripts V and L indicate the vapor and liquid phases, the subscripts ∞ and s indicate the ambient and the droplet surface, c_p is the constant pressure specific heat, T is the temperature, ρ is the density, k is the thermal conductivity, h_{LV} is the latent heat of vaporization, $\dot{Q}_L$ is the heat transferred into the droplet, and $\dot{m}$ is the instantaneous vaporization rate. We note that under the assumption of unity Lewis number (an excellent assumption here), $k^V/c_p^V = \rho^V \delta^V$, where δ^V is the self diffusion coefficient of the vapor, allowing Eq. (5) to be written in another commonly used form.[3,28] We compare the MD predictions and D^2 law calculations of the evaporation rate during the portion of the droplet lifetime

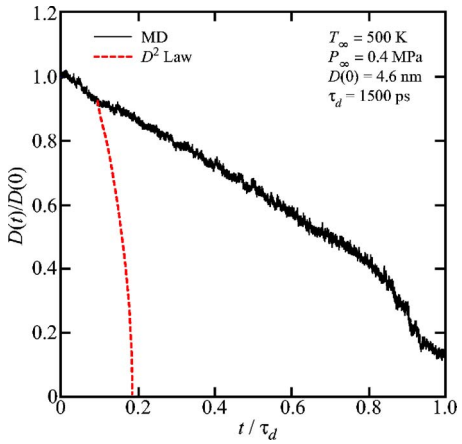

FIG. 4. (Color online) Time history of the droplet diameter predicted from the MD simulations and calculated by the D^2 law for the ambient temperature and pressure case of 500 K and 0.4 MPa.

spent in the pseudowet-bulb condition. During this period, the droplet temperature does not change with time, and therefore, $\dot{Q}_L$ can be approximated as zero. In our calculation of K:

(1) ρ^L and h_{LV} are evaluated at the measured T_s from the results of Vrabec *et al.*[24]
(2) c_p^V is estimated as $2.5R_u$, the constant-pressure specific heat for a monatomic ideal gas (a good assumption at the simulated vapor densities).
(3) k^V is taken from Ref. 29 and evaluated at $T=T_s+(1/3)\times(T_\infty-T_s)$, an appropriate reference temperature for the evaporation of a spherical, stationary droplet.[2]

2. Low ambient pressure

At the low ambient pressure of 0.4 MPa, the droplet has a nearly uniform temperature (the difference between the droplet surface and core temperatures at the pseudoquasisteady condition is less than 2 K), the surface temperature is 81 ± 2 K (see Fig. 3), and the initial Knudsen number is 1. The time history of the droplet diameter is shown in Fig. 4 for an ambient temperature of 500 K. The droplet diameter has been normalized by its initial value and time has been normalized by the droplet lifetime. Initially, the temperature of the droplet decreases (see Fig. 2), leading to an increase in droplet density and an associated decrease in the droplet diameter. After $t/\tau_d \simeq 0.1$, the droplet diameter decreases linearly until $t/\tau_d \simeq 0.9$. After this point, there is an increase in the evaporation rate, and the droplet is fully evaporated after 1500 ps.

The linear trend of droplet diameter versus time is expected because of the large value of the Knudsen number. Long *et al.*[8] also observed a droplet diameter that decreased linearly with time in a MD simulation of an argon nanodroplet evaporating into its own vapor at an ambient temperature and pressure of 120 K and 0.4 MPa. Under these conditions, our simulations predict the droplet diameter to decrease at a rate of 0.52 m/s, within 15% of the value reported by Long *et al.*

TABLE I. Evaporation rates predicted from the MD simulations at various ambient temperatures and pressures.

T_∞(K)	P_∞(MPa)	T_s(K)	dD/dt(m/s)
120	0.4	83.5	−0.52
300	0.4	82.0	−1.6
400	0.4	80.3	−1.8
500	0.4	81.2	−2.2
500	0.6	84.5	−3.5
500	0.8	89.9	−4.9
600	0.4	79.9	−2.3
700	0.4	80.6	−2.4
800	0.4	80.2	−2.5

The evaporation behavior predicted by the D^2 law is compared to our MD predictions in Fig. 4. The D^2 law overpredicts the simulated evaporation rate due to the invalidity of the continuum assumption. This overprediction is expected because hydrodynamic-based models always predict a larger evaporation rate than kinetic theory-based models.[30] The droplet evaporation in this case is strong (i.e., the vapor velocity is close to the speed of sound). We are unaware of kinetic theory-based models that are valid for the conditions of strong evaporation for such small radius nanodroplets. We provide the predicted evaporation rates in Table I for cases where the droplet diameter decreased linearly with time in order to allow others to make comparisons with our data. We estimate the uncertainty in the reported evaporation rates to be ±15% based on the scatter observed in the five independent simulations run for each case.

3. Moderate ambient pressure

At the moderate ambient pressure of 3.0 MPa, we observe that the square of the droplet diameter decreases linearly with time. At this ambient pressure, the droplet surface temperature is 113 ± 2 K (see Fig. 3), the difference between the droplet surface and core temperature is 3 ± 2 K, and the initial Knudsen number is 0.1. The ambient temperature of 500 K case is shown in Fig. 5(a). The square of the droplet diameter has been normalized by its initial value and time has been normalized by the droplet lifetime. The square of the droplet diameter initially increases due to droplet heating and then begins to decrease after $t/\tau_d \simeq 0.2$ with a linear trend developing after $t/\tau_d \simeq 0.5$. The prediction obtained from the D^2 law [also shown in Fig. 5(a)] is in excellent agreement with the MD prediction. As shown in Fig. 5(b), however, the MD predictions of the evaporation constant (calculated during the period where D^2 decreases linearly with time) do not have the nearly linear dependence on ambient temperature that is predicted by the D^2 law. Consequently, we believe the good agreement observed at an ambient temperature of 500 K to be a fortuitous result. The lack of agreement between the MD and D^2 law predicted trends may be due to the Knudsen number still being too large to approximate the vapor as a continuum.

We note that Little[9] and Walther and Koumoutsakos[7] independently concluded that their MD and D^2 law predictions were in agreement at an ambient temperature and pres-

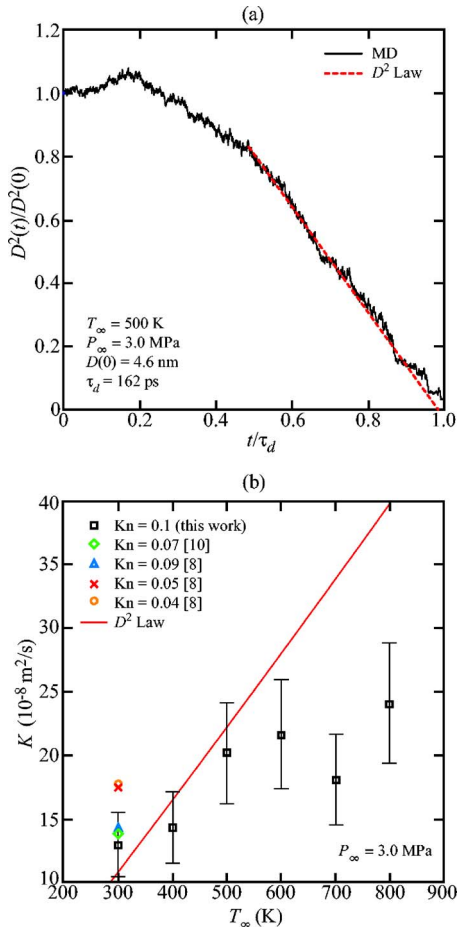

FIG. 5. (Color online) (a) Time history of the droplet diameter predicted from the MD simulations and calculated by the D^2 law for the ambient temperature and pressure case of 500 K and 3.0 MPa. (b) Droplet evaporation constant (K) predicted by the MD simulations and calculated from the D^2 law vs ambient temperature at an ambient pressure of 3.0 MPa.

sure of 300 K and 3.0 MPa. The predictions obtained by these authors are shown in Fig. 5(b). We note that these authors calculated the evaporation constant from the D^2 law to be 60%–70% greater than our D^2 law calculation. This difference is mainly due to the fact that the vapor density and the self-diffusion coefficient were evaluated at the ambient temperature rather than the more appropriate reference temperature given by the "1/3 rule."[2] It is possible that these authors would have reached a different conclusion if the appropriate reference temperature had been used or the predictions were made over a range of ambient temperatures as done here.

Altogether different evaporation behavior was observed by Sumardiono and Fischer[10] for argon nanodroplets evaporating into their own vapor at an ambient temperature and pressure of 120 K and 1.3 MPa with an initial Knudsen number of 0.5. These authors found the variation of the droplet diameter over time to be

$$D^\gamma = c - dt, \tag{6}$$

where γ, c, and d are constants. The value of γ was reported to be 3.0 when the Amsterdam method was used to determine the droplet size (a larger value of 4.5 was found using an alternative method). This is an unexpected result because

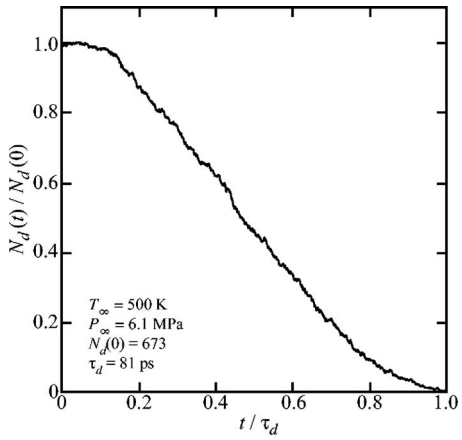

FIG. 6. Time history of the number of atoms in the droplet (N_d) for the ambient temperature and pressure case of 500 K and 6.1 MPa.

the hydrodynamic and kinetic theories predict γ to be 2 and 1. We believe that Sumardiono and Fischer's result is due to the small simulation cell they used and the lack of ambient pressure control, which allowed the ambient pressure to increase by a factor of 2.5 over the course of the simulation. This observation is based on the increase in ambient vapor density reported in Fig. 2 of their paper. An increase in the ambient pressure increases the frequency of collisions between vapor and liquid atoms, dislodging an increased number of atoms from the droplet. This dependence between the evaporation rate and ambient pressure is also predicted by kinetic theory[1,4] and confirmed from our simulation results (see the evaporation rates provided for the ambient temperature of 500 K in Table I).

4. High ambient pressure

At the high ambient pressure of 6.1 MPa, the evaporation is supercritical. Because the droplet surface temperature is above the critical temperature (see Fig. 2), our procedure to estimate the Knudsen number (described in Sec. III B 1) is not valid. The vapor density, however, is greater than the vapor density for the moderate pressure case and we believe that the evaporation occurs in the continuum regime. Also, because there is no surface tension for droplet surface temperatures above the critical temperature, the droplet has a tendency to loose its sphericity. Similar behavior has been previously observed in MD simulations of supercritical nanodroplet evaporation.[9,12,13] Because the diameter is not defined for these droplets, we describe the evaporation behavior in terms of the time evolution of the number of atoms in the droplet. The ambient temperature case of 500 K is shown in Fig. 6. The number of atoms in the droplet has been normalized by its initial value and time has been normalized by the droplet lifetime. For the majority of the droplet lifetime (i.e., between $t/\tau_d \simeq 0.2$ and $t/\tau_d \simeq 0.8$), the number of atoms in the droplet decreases at a constant rate. This trend is different than that observed by Little[9] who found that $N_d^{2/3}$ decreased linearly with time for an ambient temperature and ambient pressure of 200 K and 7.5 MPa. We find that the flux of atoms away from the droplet decreases after $t/\tau_d \simeq 0.8$,

possibly due to the decreasing droplet surface area and liquid density (which results from the increasing droplet temperature).

IV. SUMMARY AND CONCLUSIONS

Molecular dynamics simulations have been used to investigate the evaporation of argon nanodroplets into their own vapor for ambient temperatures ranging between 2.3 and 6.1 times the critical temperature and ambient pressures between 0.1 to 1.5 times the critical pressure. This range of ambient temperatures and pressures allowed the observation of the transitions from (i) high to low Knudsen number and (ii) subcritical to supercritical evaporation.

A technique for maintaining a constant ambient pressure was introduced. Such a control is necessary to be able to accurately specify the ambient conditions and examine their effects on the droplet evaporation behavior. When the ambient pressure is less than 1.4 times the critical pressure, the evaporation is subcritical and the droplet surface temperature reaches a pseudowet-bulb condition. Above this pressure, the evaporation is supercritical and the droplet surface temperature is transient over the entire droplet lifetime (see Fig. 2).

The evaporation behavior was described in detail for an ambient temperature of 500 K and low, moderate, and high ambient pressures of 0.4, 3.0, and 6.1 MPa. At the low ambient pressure, the initial droplet Knudsen number is 1, and the droplet diameter decreases linearly with time, consistent with the predictions of kinetic theory (see Fig. 4). At the moderate ambient pressure, the initial droplet Knudsen number is 0.1, and the square of the droplet diameter decreases linearly with time, consistent with hydrodynamic theory predictions (see Fig. 5). The nearly linear increasing trend of the evaporation constant with ambient temperature predicted by the D^2 law, however, is not observed in the simulation due to the droplet Knudsen number being to high to approximate the vapor as a continuum. At the high ambient pressure, the evaporation is supercritical and the flux of atoms away from the droplet is constant over the majority of the droplet lifetime.

ACKNOWLEDGMENTS

This work was supported by a National Science Foundation Graduate Research Fellowship (E.S.L.), Summer Undergraduate Research Fellowship grants from Ford Motor Co. (S.M.) and the Carnegie Mellon Undergraduate Research Office (M.P.), and the Berkman Faculty Development Fund at Carnegie Mellon University.

[1] A. Frohn and N. Roth, *Dynamics of Droplets* (Springer, Berlin, 2000).
[2] G. M. Faeth, Prog. Energy Combust. Sci. **3**, 191 (1977).
[3] W. A. Sirignano, *Fluid Dynamics and Transport of Droplets and Sprays* (Cambridge University Press, Cambridge, 1999).
[4] A. P. Kryukov, V. Y. Levashov, and S. S. Sazhin, Int. J. Heat Mass Transfer **47**, 2541 (2004).
[5] V. Chernyak, J. Aerosol Sci. **26**, 873 (1995).
[6] S. D. Givler and J. Abraham, Prog. Energy Combust. Sci. **22**, 1 (1996).
[7] J. H. Walther and P. Koumoutsakos, J. Heat Transfer **123**, 741 (2001).
[8] L. N. Long, M. M. Micci, and B. C. Wong, Comput. Phys. Commun. **96**, 167 (1996).
[9] J. K. Little, Ph.D. thesis, The Pennsylvania State University, 1996.
[10] S. Sumardiono and J. Fischer, Microfluid. Nanofluid. **3**, 127 (2007).
[11] A. P. Bhansali, Y. Bayazitoglu, and S. Maruyama, Int. J. Therm. Sci. **38**, 66 (1999).
[12] T. L. Kaltz, L. N. Long, M. M. Micci, and J. K. Little, Combust. Sci. Technol. **136**, 279 (1998).
[13] L. Consolini, S. K. Aggarwal, and S. Murad, Int. J. Heat Mass Transfer **46**, 3179 (2003).
[14] S. Sumardiono and J. Fischer, Int. J. Heat Mass Transfer **49**, 1148 (2006).
[15] N. W. Ashcroft and N. D. Mermin, *Solid State Physics* (Sauders College, Fort Worth, 1976).
[16] J. R. Lukes, D. Y. Li, X.-G. Liang, and C.-L. Tien, J. Heat Transfer **122**, 536 (2000).
[17] A. R. Abramson, C.-L. Tien, and A. Majumdar, J. Heat Transfer **124**, 963 (2002).
[18] J.-L. Barrat and F. Chiaruttini, Mol. Phys. **101**, 1605 (2003).
[19] Y. Chen, D. Li, J. R. Lukes, Z. Ni, and M. Chen, Phys. Rev. B **72**, 174302 (2005).
[20] A. J. H. McGaughey and M. Kaviany, Int. J. Heat Mass Transfer **47**, 1783 (2004).
[21] A. J. H. McGaughey and M. Kaviany, Phys. Rev. B **69**, 094303 (2004).
[22] A. J. H. McGaughey, M. I. Hussein, E. S. Landry, M. Kaviany, and G. M. Hulbert, Phys. Rev. B **74**, 104304 (2006).
[23] J. A. Thomas and A. J. H. McGaughey, J. Chem. Phys. **126**, 034707 (2007).
[24] J. Vrabec, G. K. Kedia, G. Fuchs, and H. Hasse, Mol. Phys. **104**, 1509 (2006).
[25] P. R. ten Wolde and D. Frenkel, J. Chem. Phys. **109**, 9901 (1998).
[26] L. B. Loeb, *The Kinetic Theory of Gases* (Dover, New York, 1961).
[27] B. Abramzon and W. A. Sirignano, Int. J. Heat Mass Transfer **32**, 1605 (1989).
[28] S. R. Turns, *An Introduction to Combustion: Concepts and Applications* (McGraw-Hill, Singapore, 2000).
[29] R. C. Reid, J. M. Prausnitz, and B. E. Poling, *The Properties of Gases and Liquids* (McGraw-Hill, New York, 1987).
[30] S. S. Sazhin, I. N. Shishkova, A. P. Kryukov, V. Y. Levashov, and M. R. Heikal, Int. J. Heat Mass Transfer **50**, 2675 (2007).